DIFFUSION-REACTION MODEL FOR ALKALI-SILICA REACTION IN CONCRETE

JOAQUÍN LIAUDAT*, CARLOS M. LÓPEZ AND IGNACIO CAROL

ETSECCPB (School of Civil Engineering -Barcelona)
UPC (Technical University of Catalonia)
Jordi Girona, 1, Edif D2, E-08034 Barcelona
Email: joaquin.liaudat@upc.edu, carlos.maria.lopez@upc.edu, ignacio.carol@upc.edu

Key words: Concrete, ASR, Diffusion Reaction, Reactive transport, Numerical Modeling

Abstract. A new diffusion-reaction model for the potentially deleterious Alkali-Silica Reaction (ASR) process in concrete is presented. The model involves three coupled diffusion processes, two in-going and one out-going from the aggregate viewpoint. Alkali (Na^+ and K^+) and Calcium (Ca^{2+}) ions diffuse "inwards", from high molar concentration sites in the pores of the cement paste phase of the concrete specimen or at its boundaries, towards the aggregate-cement paste interfaces or the inner cracks of the aggregates. The OH^- ions associated with alkali and calcium ions attack certain forms of silica in the aggregates (the "reactive silica"), dissolving it in the form of silicate ions which in turn diffuse back to the cement paste phase ("outwards"). The final potentially deleterious ASR precipitation process involves those silicate ions, plus calcium and alkalis. It takes place wherever the reactants are available by precipitating silicate hydrates of two kinds (Calcium-Silicate-Hydrates –CSH or Calcium-Alkali-Silicate-Hydrates –CASH) in a proportion depending on concentrations and temperature. The diffusion-reaction equations of this process are discretized in space and time using finite differences. An example of application in 1D is presented to illustrate the capabilities to reproduce realistically the ASR process, including some novel features not usually which are not considered in the available literature, such as the role of calcium in the development of the reaction and the inherent relationship between the reaction product composition and its swelling capacity.

1 INTRODUCTION

Expansion due to Alkali Silica Reaction (ASR) is the second most common cause of concrete deterioration, after reinforcement corrosion. First reported by Stanton in 1940 [1], its reaction-expansion mechanism is not yet fully understood. It is accepted that certain types of metastable silica present in aggregates are attacked by hydroxyl ions in concrete pore solution producing its dissolution into silicate ions. These ions recombine with alkalis and calcium ions in an expansive reaction forming a Calcium-Alkali-Silicate-Hydrates (CASH) of variable stoichiometry, molar volume and mechanical properties. It is a complex phenomenon that strongly depends on the dosage and composition of the concrete, as well as on its temperature and capillary pore humidity.

ASR products are found filling pores and cracks both in the hydrated cement paste (HCP)

and the aggregates of concrete. However, the most expansive ASR products seem to be those with low content of calcium, formed in aggregate cracks or pockets were calcium from the HCP is less available. On the other hand, the presence of calcium appears to be essential for concrete expansion [2], as Portlandite ($Ca(OH)_2$) in the HCP acts as a buffer to maintain the OH^- concentration in the pore solution at high values, therefore allowing further dissolution of the reactive silica [3].

Some chemo-mechanical simulations of ASR have been reported in the last fifteen years [4, 5, 6]. To the best of the authors' knowledge, only Poyet et al. [7] have considered the role of portlandite and calcium ions diffusion in the development of ASR. However, they have neglected the silicate ions diffusion by assuming that the ASR products only precipitate in the interfacial transition zone surrounding the reactive aggregate.

In this paper, diffusion-reaction model currently under development is presented. It includes three diffusion processes: alkali and calcium ions, mainly from the HCP into the aggregate, and silicate ions, mainly from the aggregates towards the HCP. The main objective is to reproduce realistically some aspects of ASR which are not considered in the available models, such as the role of calcium in the development of the reaction and the inherent relationship between the reaction product composition and its swelling capacity. For the sake of simplicity, constant temperature and full water saturation of concrete are assumed at this stage of the formulation development. For validation purposes, the model has been implemented in 1D and compared with experimental results of free expansion tests at the level of a single cement-aggregate interface taken from an ongoing experimental campaign within the same study.
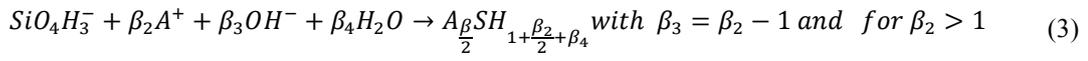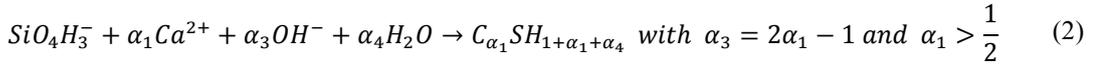
2 DESCRIPTION OF THE CHEMO-TRANSPORT MODEL

2.1 Chemical reactions involved

Chemical reactions leading to ASR expansions occur in the pore water of the cement paste and aggregate phases in concrete. When pore solution of usually high pH is in contact with metastable silica present in the aggregate, an acid-base reaction takes place, leading to the dissolution of the silica into silicate ions [8]. This reaction involves the progressive dissociation of the silicate ions, and can be expressed in a simplified way [9] as:

$$SiO_2, H_2O_{(surf.)} + OH^- \rightarrow SiO_4H_3^-(aq) \tag{1}$$
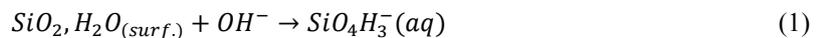
Once in the pore solution, the silicate ions react with calcium and alkali ions forming a Calcium-Alkali-Silicate-Hydrate gel (CASH) of variable stoichiometry depending on the relative concentration of the reactants [10, 11]. The variability of the stoichiometry seems to be an important issue, since a clear dependence of the molar volume and the mechanical properties of the CASH on its composition, particularly with the Calcium to silica ratio has been reported [11, 12]. In order to include this effect, the model considers the following two simultaneous reactions, one (2) forming a Calcium- Silicate – Hydrate (CSH) and the other (3) forming a Calcium-Alkali-Silicate-Hydrate (CASH), where α_1, α_3, α_4 and β_2, β_3, β_4 are stoichiometric coefficients to be fit with experimental data. The overall product of the reaction is dependent on the kinetics of CASH and CSH formation.

$$SiO_4H_3^- + \alpha_1 Ca^{2+} + \alpha_3 OH^- + \alpha_4 H_2O \rightarrow C_{\alpha_1}SH_{1+\alpha_1+\alpha_4} \ with \ \alpha_3 = 2\alpha_1 - 1 \ and \ \alpha_1 > \frac{1}{2} \quad (2)$$

$$SiO_4H_3^- + \beta_2 A^+ + \beta_3 OH^- + \beta_4 H_2O \rightarrow A_{\frac{\beta}{2}}SH_{1+\frac{\beta_2}{2}+\beta_4} \ with \ \beta_3 = \beta_2 - 1 \ and \ for \ \beta_2 > 1 \quad (3)$$

The prediction of the chemical composition of concrete pore water is a very complex problem [13]. However, in this study cement pore water is assumed to be a solution of Na^+, K^+, Ca^{2+} and OH^- ions, where portlandite $(Ca(OH)_2)$ solubility controls Ca^{2+} concentrations [14]. Since $NaOH$ and KOH are strong bases, it can be assumed that all of it is dissociated, i.e. no solid $NaOH$ or KOH is in contact with the pore solution. Finally, only two dissociation reactions are considered: water self-ionization (4) and portlandite dissociation (5).

$$H_2O + H_2O \leftrightarrow OH^- + H_3O^+ \quad (4)$$

$$Ca(OH)_2 \leftrightarrow Ca^{2+} + 2(OH)^- \quad (5)$$

Since Na^+ and K^+ have similar effects on ASR, henceforth they are called generically A^+.

2.2 Transport processes

The preceding chemical reactions take place according to the availability of reactants in time and space which is basically determined by transport processes. In this model, only the diffusion of Ca^{2+}, A^+ and $SiO_4H_3^-$ are explicitly modeled. The OH^- and OH_3^+ concentrations are obtained at each location by means of the chemical equilibrium equations above mentioned. These diffusion processes are formulated by means of Fick's second law, which is expressed in 1D for ion $SiO_4H_3^-$ in equation (6), where $s^- \ [mol/m^3]$ is the ion concentration, $D^s \ [m^2/h]$ is the overall diffusion coefficient (see section 2.3) and $\dot{s}^- [mol/(m^3 \cdot h)]$ is a well/sink term which accounts for the net production or consumption due to chemical processes of the ionic species s^-.

$$\frac{\partial s^-}{\partial t} = \frac{\partial}{\partial x}\left(D^s \frac{\partial s^-}{\partial x}\right) + \dot{s}^- \quad (6)$$

Similar equations are assumed for ions Ca^{2+} (concentration c^{2+}) and A^+ (concentration a^+). The notation used for the independent variables is also stated in Table 1.

2.3 Volume fractions of solid components

During the development of the reaction the volume fractions of the solid components in the material are not constant. Portlandite and reactive silica are progressively dissolved reducing their volumes and increasing the capillary porosity of the material. The CASH formed occupies this empty volume, leading to a net volumetric expansion when the volume of CASH produced exceeds the available pore space.

Eight different solid components are considered in this model:

1) *Impervious remnant*: comprises impervious and inert constituents in HCP and aggregate. There is no diffusion through it and it does not experiment any volume change.

2) *Capillary pores*

3) *Reactive silica*

4) *Portlandite*

5) *Reaction product (CSH):* product of reaction (2),

6) *Reaction product (CASH):* product of reaction (3)

7) *Inert cement hydration products:* comprises cement paste constituents that do not take part in the reactions above mentioned. It does not experiment any volume change due to ASR.

8) *Inert aggregate constituents:* comprises aggregate constituents that do not take part in the reactions above mentioned. It does not experience any volume change due to ASR.

Components 1, 2, 4 and 7 are initially present in the HCP. Components 1, 2, and 8 are initially present in the aggregates. Components 5 and 6 precipitate both in the HCP and in the aggregates as the reaction takes place.

At a given location in space x, the volume fraction of each component k is represented by a variable $u_k(x)$, so that the total volume $V(x)$ is given by equation (7).

$$V(x) = \sum_{k=1}^{8} u_k(x) \tag{7}$$

The volume fractions $u_k(x)$ are calculated from the concentration variables by means of equations (8), (9) and (10), where v_k is the molar volume and $c_k(x)$ is the concentration of the chemical species associated to the component k (e.g. for portlandite $k = 4$, $c_4 = c^0$). The superindex 0 applied to $u_k(x)$ stands for initial value.

$$u_k(x) = u_k^0(x) \quad for \ k = 1,7,8 \tag{8}$$

$$u_2(x) = \max\left\{0 \ ; \ u_2^0(x) - \sum_{k=2}^{6} [u_k(x) - u_k^0(x)]\right\} \tag{9}$$

$$u_k(x) = v_k \cdot c_k(x) \cdot V_{ps}(x) \quad for \ k = 3,4,5,6 \tag{10}$$

The volumetric distribution of the solid components in each location determines the volume of pore solution $V_{ps}(x)$ in it by equation (11) and its overall diffusion coefficients by equation (12) (similar equations are posed for $D^a(x)$ and $D^s(x)$) where φ_k and d_k are the intrinsic porosity and the diffusion coefficient of phase k, and m_s is a coefficients that introduces the effect of the ion type (electric charge, ionic radius). The intrinsic porosity is defined as the volumetric fraction of the phase occupied with physically bonded water through which the diffusion-reaction process can happen.

$$V_{ps}(x) = \sum_{k=1}^{6} u_k(x) \cdot \varphi(k) \tag{11}$$

$$D^s(x) = \frac{m_s}{V(x)} \sum_{k=1}^{8} u_k(x) \cdot d_k \tag{12}$$

2.4 Chemical equations

The set of chemical reactions described in section 2.1 is divided in two groups depending

on their kinetics. The first group includes water self-ionization (4) and portlandite dissociation (5), reactions that can be assumed to occur instantaneously. The second group involves slower reactions for which kinetic laws need to be established such as silica dissolution (1) and CSH/CASH formation (2) and (3).

The equilibrium equations for the first group are:

$$K_w = \{H_3O^+\}\{OH^-\} = \gamma_{h^+} \cdot \gamma_{oh^-} \cdot h^+ \cdot oh^- \tag{13}$$

$$K_3^{sp} = \{Ca^{2+}\}\{OH^-\}^2 = \gamma_{c^{2+}} \cdot (\gamma_{oh^-})^2 \cdot c^{2+} \cdot (oh^-)^2 \tag{14}$$

in which K_w and K_3^{sp} are constants, and activity coefficients γ_{h^+}, γ_{oh^-} and $\gamma_{c^{2+}}$ are used instead of mere ion concentrations, for a more realistic representation. Activity coefficients are obtained from Davies equation (15), where A is the Debye-Hückel parameter, z_n is the electric charge of the ion and I is the ionic strength of the solution. The ionic strength is calculated from (16), where c_n is the molar concentration of the ion species n.

$$\log_{10} \gamma_n = -Az_n^2 \left(\frac{\sqrt{I}}{1+\sqrt{I}} - 0.2I \right) \tag{15}$$

$$I = \frac{1}{2} \sum_n c_n |z_n|^2 \tag{16}$$

Davies equation gives realistic values of activity coefficients for $I<0.50$. For greater ionic strength other method should be used (p.e. Pitzer equations). However, for the sake of simplicity, Davies Equation is used in the full range of ionic strength, even over 0.50.

Additionally, electric charge balance (17) and calcium mass balance equations (18) need to be considered to obtain the equilibrium composition of the pore solution.

$$\sum_i c_n z_i = 0 \tag{17}$$

$$c^{2+} + c^0 - c_0^{2+} - c_0^0 = 0 \tag{18}$$

For the second group of reactions, kinetics laws of order zero are assumed for silica dissolution (19), CSH formation (20) and CASH formation (21), where k_1, k_4, k_5 are kinetic constants. In equation (19), a term has been added to limit the silica dissolution to its saturation product K_1^{sp}. In turn, if oversaturation is reached, this term allows silica precipitation.

$$\frac{\partial s^-}{\partial t} = k_1 \cdot s^0 \cdot s^- \cdot \left(1 - \frac{s^-}{oh^- \cdot K_1^{sp}} \right) \tag{19}$$

$$\frac{\partial csh}{\partial t} = k_4 \cdot s^- \cdot (c^{2+})^{\alpha_1} \cdot (oh^-)^{\alpha_3} \tag{20}$$

$$\frac{\partial cash}{\partial t} = k_5 \cdot s^- \cdot (a^+)^{\beta_2} \cdot (oh^-)^{\beta_3} \tag{21}$$

The amount of reaction products and the pore solution composition for a given time interval is obtained by posing the mass balance equations for s^0, s^-, c^{2+}, a^+ and oh^-. The

notation used for the independent variables is also stated in Table 1.

Table 1: Summary of independent calculation variables.

Notation	Units	Description	Notes
s^0, S^0	–	Molar concentration of reactive silica SiO_2	(a), (c)
c^0, C^0	–	Molar concentration of Portlandite $Ca(OH)_2$	(a), (c)
s^-	–	Molar concentration of silicate ions $SiO_4H_3^-$	(b), (d)
c^{2+}	–	Molar concentration of calcium ions Ca^{2+}	(b), (d)
a^+	–	Molar concentration of alkali ions Na^+ and K^+	(b), (d)
oh^-	–	Molar concentration of hydroxyl ions OH^-	(b), (d)
h^+	–	Molar concentration of hydroxyl ions H^+	(b), (c)

Notes: (a) Solid species, expressed in terms of pore solution volume (low case) and in terms of initial unitary volume of concrete (upper case). (b) Species in solution, expressed in terms of pore solution volume. (c) Local variable (d) Field variable.

3 SUMMARY OF EQUATIONS AND NUMERICAL IMPLEMENTATION

In sum, the overall system of unknowns and equations to be solved in the ASR model proposed is the following:

- Three equations of diffusion/reaction (6) for c^{2+}, a^+ and s^-. They are the only field variables of the problem.
- For each point in space, the sink/well terms of Eqns. (6) and local concentration variables ($oh^-, h^+, c^0, s^0, csh, cash$) are calculated by means of:
  o Four Chemical Equilibrium equations
    - Electric charge balance equation (17)
    - Water dissociation equilibrium equation (13)
    - Saturation product of Portlandite dissolution (14)
    - Molar mass balance of portlandite dissolution (18)
  o Three Chemical Kinetic equations
    - Silica dissolution (19)
    - CSH formation (20)
    - CASH Formation (21)

Additionally, the overall diffusion coefficients $D^a(x)$, $D^c(x)$, $D^s(x)$ and the pore solution volume $V_{ps}(x)$ are related to the volume fractions $u_k(x)$ by equations (11, 12), as well as the volume fractions $u_k(x)$ are related to the local concentration variables c^0, s^0, csh and $cash$ by equations (8, 9,10).

The solution scheme implemented is as follow:
- Time is discretized in $\Delta t = t_{j+1} - t_j$
- Space is discretized in segments of variable length $\Delta x_i = x_{i+1} - x_i$
- For each time step, the initial concentrations $C_n(x_i)$ (expressed in relation to the initial unit volume) and volume fractions $u_k(x_i)$ at each point x_i are known.
- With the volume fractions $u_k(x_i)$, the diffusion coefficients $D_n(x_i)$ and pore solution volumes $V_{ps}(x_i)$ are calculated by equations (11, 12).
- Concentrations are expressed in terms of pore solution volume by means of
  $c_n(x_i) = C_n(x_i)/V_{ps}(x_i)$
- Time derivatives of Eqns. (6) are evaluated at $t = t_j$ by the explicit finite difference method. Sink/well terms of Eqns. (6) are obtained by combining the equilibrium equations (13, 14, 17, 18) and the kinetics equations (19, 20, 21). The equilibrium equations are established at $t = t_{j+1}$, while the kinetics equations are discretized in Δt by a mid-point integration scheme
- The resulting equation system for concentrations at time $t = t_{j+1}$ is solved by means of Newton-Raphson method.
- Concentrations at $t = t_{j+1}$ are saved for the next time step.

4 1D SIMULATIONS

In order to validate the reaction mechanism proposed, an ongoing experimental test similar to the one proposed by Schlangen and Çopuroglu [15] is simulated. The test has been set up to measure ASR expansions at the level of single interfase between HCP and aggregate. Cylindrical specimens of 33 mm of diameter and 64 mm of height, with a borosilicate glass disc in the middle as reactive aggregate and HCP in the extremes (see Figure 1, left) are exposed to a 1M NaOH solution at 60ºC for a period of 14 days during which expansions are measured regularly.
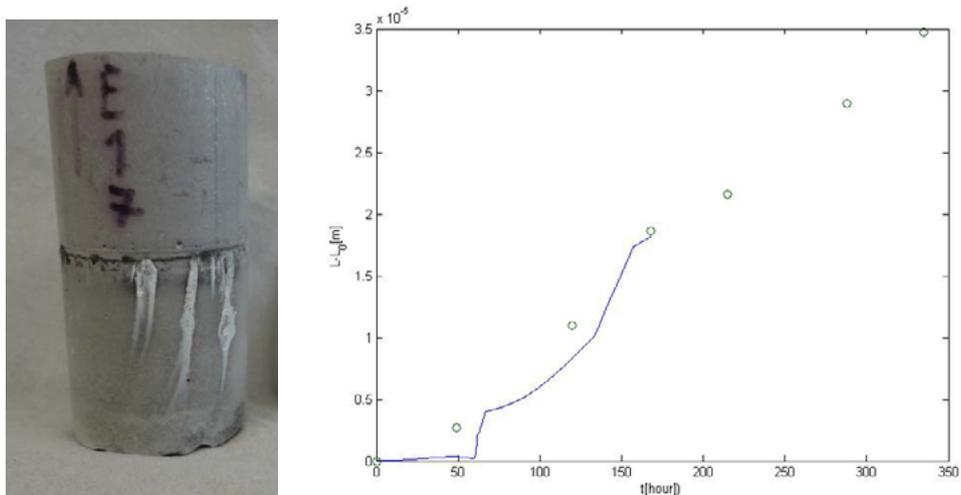

Figure 1: Experimental ASR expansion test at the level of a single aggregate-HCP interface: specimen after 14 days imersion in 1M NaOH solution at 60ºC (left image), and length change from experiment (circles) and model (line) (right diagram).

The geometry and discretization for the 1D numerical analysis are is shown in Figure 2. A total of 200 nodes were used with a constant separation of 5.0E-06m. The boundary and initial conditions as well as the parameters and coefficients used in the simulations are summarized in Tables 2, 3 and 4. A symmetric boundary condition is imposed on the right end.
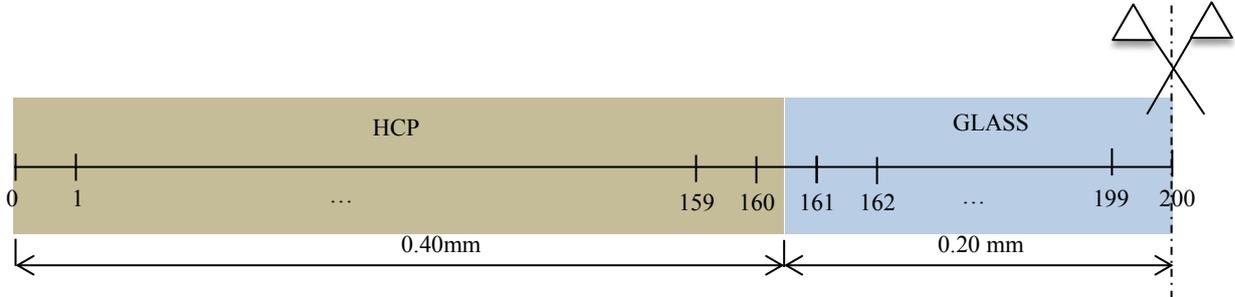

Figure 2: Model geometry and discretization (not represented at exact scale).

Table 2: Constants and coefficients used in the simulation.

K_w	9.43E-14	k_1	2.00E+02	m_c	0.75	α_1	0.50
K_1^{sp}	1.00E+05	k_4	2.00E+03	m_c	1.25	α_2	0.00
K_3^{sp}	4.60E-06	k_5	2.00E+00	m_s	1.00	β_1	1.00
A	5.49E-01					β_2	0.00

Table 3: Intrinsic properties of the solid phases (SP).

	Unit	SP 1	SP 2	SP 3	SP 4	SP 5	SP 6	SP 7-8
d_k	m²/h	0.00E+00	1.00E-07	1.00E-12	1.00E-11	1.00E-09	1.00E-09	1.00E-11
φ_k	--	1.00E-01	1.00E+00	0.00E+00	1.00E-03	1.00E-01	1.00E-01	1.00E-01
v_k	10^{-3}m³/mol	N/A	N/A	2.87E-02	3.32E-02	5.68E-02	8.56E-02	N/A

Table 4: Initial conditions

	u_2	S^0	S^-	C^0	C^{2+}	A^+
Unit	m³/m³	10^3 mol/m³	10^3 mol/m³	10^3 mol/m³	10^3 mol/m³	10^3 mol/m³
HCP	0.18	1.00E+00	0.00E+00	3.3800E+00	1.93E-06	4.43E-01
GLASS	0.00	2.78E+01	0.00E+00	0.0000E+00	0.0000E+00	0.00E+00
Left boundary	0.18	0.00E+00	0.00E+00	3.3800E+00	1.93E-06	4.43E-01

The overall expansion curve obtained with the model is plotted together with the experimental results in Figure 1. The main trend of experimental behavior is caught by the model.

The volumetric solid phase distribution in the area near the HCP-glass interface, for different exposure times, is represented in Figure 3. There, the progressive glass and portlandite depletion near the interface becomes apparent, as well as the CASH precipitation, first filling the capillary pores and finally producing a volumetric expansion.
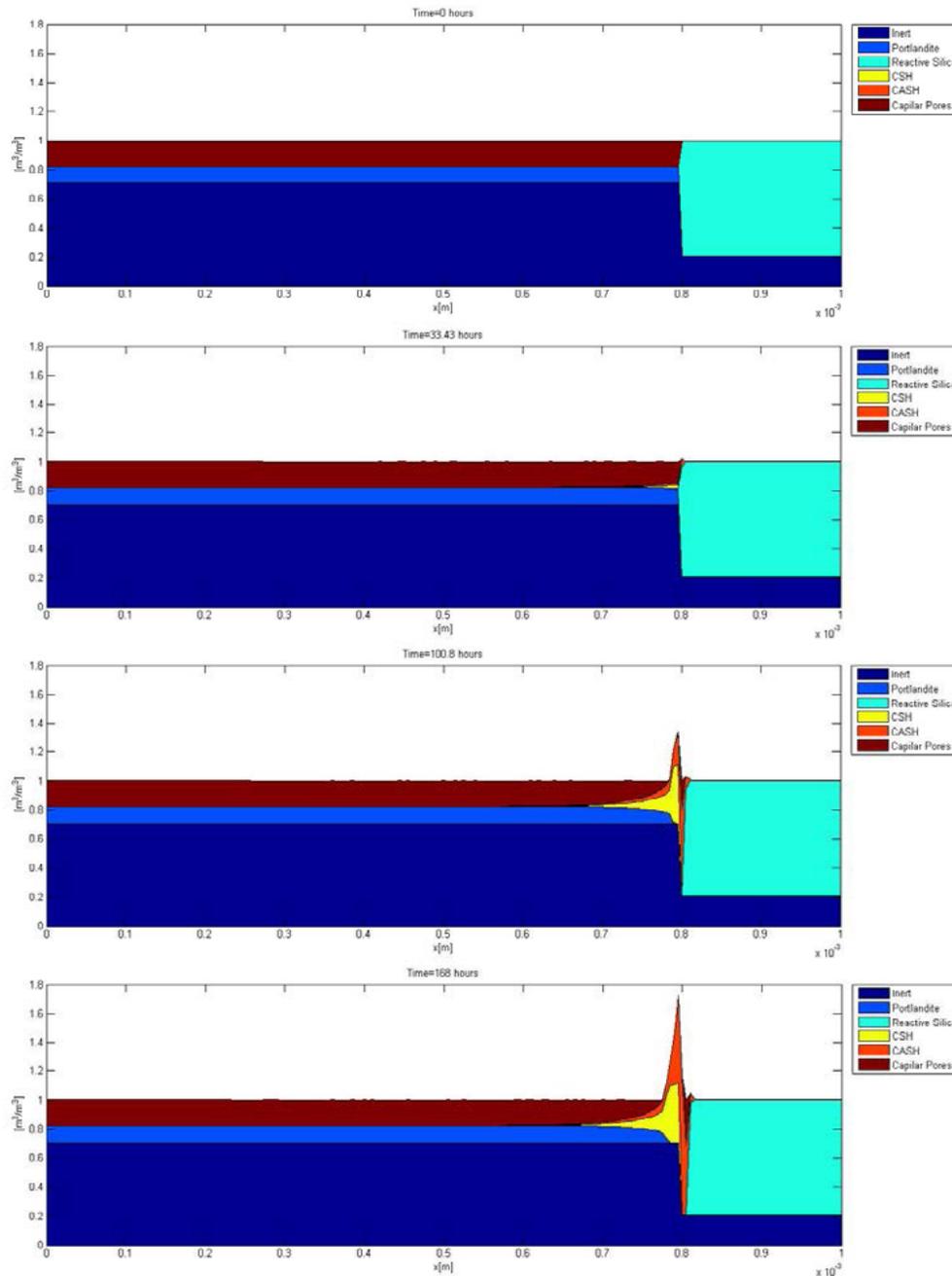

Figure 3: Volumetric solid phase distribution in the interface zone of HCP-glass for different exposure times.

4   CONCLUDING REMARKS

The model proposed is capable of qualitatively reproducing several aspects of the ASR expansion, the main ones of which:

- Calcium enrichment of the ASR product.
- Experimental expansion curves at the level of a single HCP- glass interface.
- The effect of calcium availability on the silica dissolution and development of expansions.
- Free expansion curves at the level of a single interface.
- The effect of calcium and silica dissolution and the ASR products precipitation on the overall diffusivity coefficient

Some aspects object of on-going development improvement:

- The effect of sulfate ions in the composition of pore solution at high temperatures.
- Second order effect on diffusion due to volumetric expansion.

ACKNOWLEDGEMENTS

REFERENCES

[1] Stanton, T. E. Expansion of concrete through reaction between cement and aggregate. *Proceedings of American Society of Civil Engineers* (1940) **66**: 1781-1811.

[2] Thomas, M. D. The role of calcium in alkali-silica reaction, Materials Science of Concrete (Sidney Diamond Symposium). *The American Ceramic Society Bulletin* (1998), special volume, 325-337.

[3] Wang, H., & Gillott, J. Mechanism of alkali-silica reaction and the significance of calcium hydroxide. *Cement and Concrete Research* (1991) **21**:647-654.

[4] Ulm, F.-J., Coussy, O., Kefei, L., & Larive, C. Thermo-chemo-mechanics of ASR expansion in concrete structures. *Journal of Engineering Mechanics* (2000) **126:** 233-242.

[5] Xi, Y., Suwito, A., Wen, X., Meyer, C., & Jin, W. Testing and Modeling Alkali-Silica Reaction and the Associated Expansion of Concrete. *In G. Pijaudier-Cabot, Z. Bittnar, B. Gerard, & (Editors), Mechanics of Quasi-Brittle Materials and Structures: A Volume in Honor of Prof. Z.P. Bazant's 60th Birth Day* (1999) 217-232.

[6] Xi, Y., & Suwito, A. The Effect of Microstructure Features on Pessimum Effect of ASR in Concrete. *5th World Congress on Computational Mechanics* (2002).

[7] Poyet, S., Sellier, A., B., C., Foray, G., Torrenti, J. M., Cognon, H., et al. Chemical modelling of Alkali Silica reaction: Influence of the reactive aggregate size ditribution. *Materials and Structures* (2007) **40:** 229-239.

[8] Struble, L., & Diamond, S. Influence of cement pore solution on expansion. *8th International Conference on Alkali-Aggregate Reaction* (1989), 167-172.

[9] Dron, R., & Brivot, F. Thermodynamic and kinetic approach to the alkali-silica reaction. Part 1: Concepts. *Cement and Concrete Research* (1992) **22**: 941-948.

[10] Hou, X., Struble, L. J., & Kirkpatrick, R. J. Formation of ASR gel and the roles of C-S-H

and portlandite. *Cement and Concrete Research* (2004) **34:** 1683-1696.

[11] Leemann, A., Le Saout, G., Winnefeld, F., Rentsch, D., & Lothenbach, B. Alkali–Silica Reaction: the Influence of Calcium on Silica Dissolution and the Formation of Reaction Products. *J. Am. Ceram. Soc.* (2011) **94**: 1243-1249.

[12] Leemann, A., & Lura, P. E-modulus of the alkali-silica-reaction product determined by micro-indentation. *Construction and Building Materials* (2013) **44**: 221-227.

[13] Reardon, E. J. Problems and approaches to the prediction of the chemical composition in cement/water systems. *Waste Management* (1992) **12:** 221-239.

[14] Duchesne, J. & Reardon, E. J. Measurement and prediction of portlandite solubility in alkali solutions. *Cement and Concrete Research* (1995) **25:** 1043-1053.

[15] Schlangen, E., & Çopuroglu, O. Concrete damage due to alkali-silica reaction: A new method to determine the properties of expansive gel. In Carpinteri et al. (eds.), *Fracture Mechanics of Concrete and Concrete Structures - High-Performance Concrete, Brick-Masonry and Environmental Aspects* (2007), 1835-1841. London: Taylor & Francis Group.